Bulletin of the Seismological Society of America, Vol. 107, No. 6, pp. 3044–3051, December 2017, doi: 10.1785/0120160355

Ⓔ

Short Note

The 9 September 2016 North Korean Underground Nuclear Test

by Lian-Feng Zhao, Xiao-Bi Xie, Wei-Min Wang, Na Fan, Xu Zhao, and Zhen-Xing Yao

Abstract We characterize the seismic events that occurred in North Korea on 9 September 2016 and South Korea on 12 September 2016. The 9 September 2016 event was identified as an explosion, and the two 12 September 2016 events were identified as natural earthquakes using the *P*/*S* (*P*- and *S*-wave) spectral ratios, *Pg*/*Lg*, *Pn*/*Lg*, and *Pn*/*Sn* as discriminants. The explosive event was relocated within the North Korean nuclear test site using a relative location method and the 2006 North Korea underground nuclear test as the master event, and the epicenter was identified at 41.2976° N latitude and 129.0804° E longitude. From the regional *Lg* and Rayleigh waves, the body- and surface-wave magnitudes for the 9 September 2016 event were calculated as $m_b(Lg) = 4.8 \pm 0.2$ and $M_s = 4.2 \pm 0.1$. By adopting an empirical magnitude–yield relation for the body-wave magnitude, and assuming that the explosion was fully coupled and detonated at a normally scaled depth, we estimated that the seismic yield was ~6 kt, and the uncertainty range was between 3 and 11 kt. If an overburied depth range between 780 and 1200 m was applied, then the yield would be increased to 16–22 kt.

Electronic Supplement: Figures comparing the vertical seismograms for events occurring on 9 and 12 September 2016; spectral ratios from individual stations and events; *Pn*-waveform cross correlations at selected stations and vertical Rayleigh waveforms from NKT5 recorded at station HIA; and tables of the cross-correlation parameters of the *Pn* waveforms, residuals of *Pn* differential travel times, and event parameters used in this study.

Introduction

At 00:30 (UTC) on 9 September 2016, a seismic event occurred near the North Korean nuclear test site (NKTS) (red star in Fig. 1). The North Korea government subsequently claimed that they had successfully conducted an underground nuclear test, the fifth in a series of tests conducted in 2006, 2009, 2013, and January 2016. The U.S. Geological Survey reported that the event was located at 41.32° N, 128.99° E, and that the magnitude was m_b 5.3. The waveform from the recent event is similar to those from previous nuclear tests, and they all featured abrupt primary *P* waves, relatively weak *Lg* phases and well-developed short-period Rayleigh waves (Fig. 2).

Coincidentally, two other seismic events occurred on the Korean Peninsula on 12 September 2016 (green symbols in Figs. 1 and 3a). These events were also recorded by the same seismic networks in the region. Data from the China National Digital Seismic Network, the Global Seismic Network, and Japan's F-NET are collected for this study. With which, we investigate the characteristics of the above-mentioned seismic events on the Korean Peninsula. Using the *P*/*S* spectral ratio method (e.g., Richards and Kim, 2007; Zhao *et al.*, 2008; Shin *et al.*, 2010; Murphy *et al.*, 2013), we confirm that the 9 September 2016 event was an explosion, whereas the two 12 September 2016 events were natural earthquakes. For the explosion that occurred at the NKTS, we use the relative location method (Schaff and Richards, 2004; Schlittenhardt *et al.*, 2010; Selby, 2010; Wen and Long, 2010; Murphy *et al.*, 2013; Zhang and Wen, 2013; Zhao *et al.*, 2014) to obtain its epicenter relative to that of the 2006 test, determine its body- and surface-wave magnitudes (Bonner *et al.*, 2006, 2008, 2011; Russell, 2006; Chun *et al.*, 2011; Fan *et al.*, 2013), and estimate its seismic yields (e.g., Zhao *et al.*, 2008, 2012, 2014; Murphy *et al.*, 2013; Zhang and Wen, 2013). Hereafter, we refer to these five successive North Korean nuclear tests as NKT1, 2, 3, 4, and 5.

Event Discrimination

At regional distances, because of different scalings of *P*- and *S*-wave excitation functions between explosion and

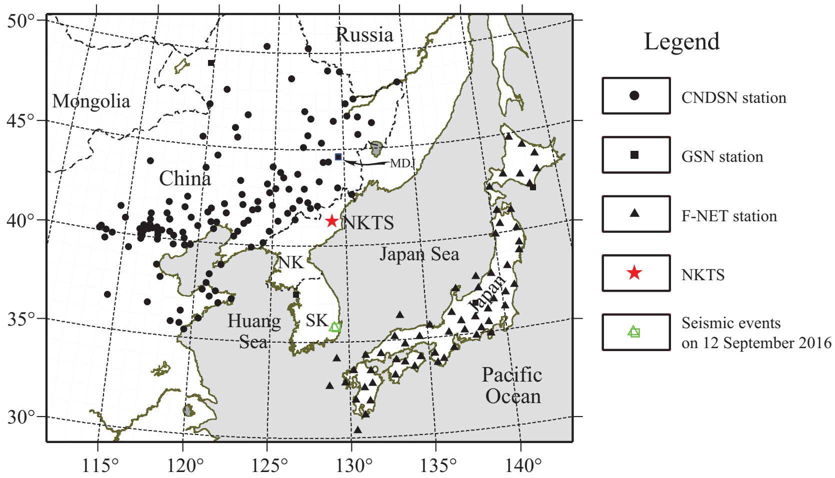

Figure 1. Map showing the locations of the North Korean nuclear test site (NKTS; red star), the China National Digital Seismic Network (CNDSN; solid circles), Global Seismic Network (GSN; solid squares), and F-NET (triangles) stations used for relocation. Station MDJ (pointed by an arrow) and two seismic events occurred on 12 September 2016 (green symbols) are also labeled. NK, North Korea; SK, South Korea.

earthquake sources, the *P*/*S*-type spectral ratio can represent an effective discriminant for identifying explosion and earthquake sources (e.g., Taylor *et al.*, 1989; Kim *et al.*, 1993; Walter *et al.*, 1995, 2007; Xie, 2002; Fisk, 2006). The source discrimination dataset for the Korean Peninsula consists of four previously confirmed North Korean explosions, four nearby earthquakes, and three recent events on 9 and 12 September 2016. For these events, we sampled the regional phases *Pn*, *Pg*, *Sn*, and *Lg* from vertical-component displacement waveforms at stations with almost purely continental paths and calculated the *P*/*S*-type spectral ratios *Pg*/*Lg*, *Pn*/*Lg*, and *Pn*/*Sn* at individual stations (Hartse *et al.*, 1997; Zhao *et al.*, 2008, 2016). The amplitude–frequency–distance corrections are derived based on the data from all 11 events (Walter *et al.*, 2007). The most prominent features are that the 9 September 2016 event has strong *Pn* and *Pg* waves at all distances, whereas the two 12 September 2016 events have more developed *Lg* waves (Ⓔ Fig. S1, available in the electronic supplement to this article). Although the two South Korea events are biased to the southeastern edge of the Korean Peninsula, these profiles appear to have similar group velocities for different regional phases. This may be because they are still located in the same geological platform. The stations used to calculate the spectral ratios are illustrated in Figure 3a. Although the spectral ratios generally separate the explosions from earthquakes, overlaps are observed in these ratios from individual stations. Illustrated in Ⓔ Figure S2

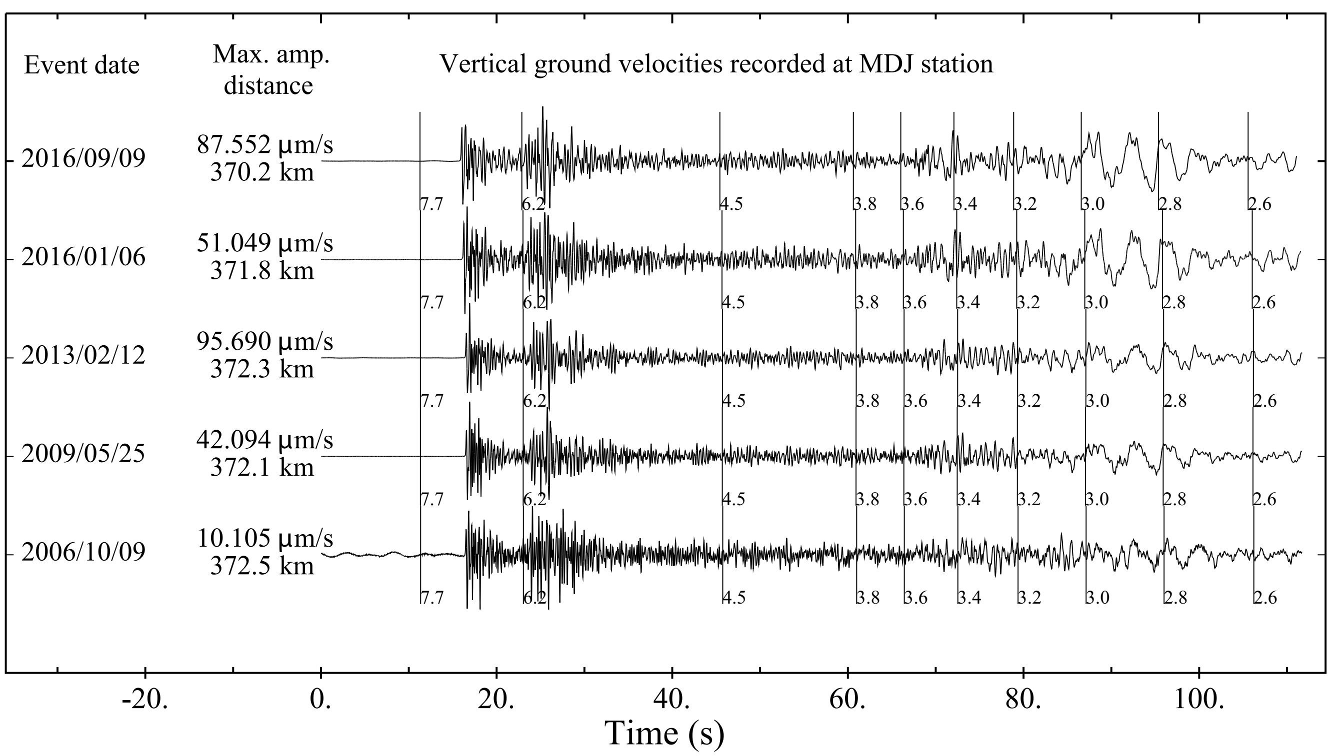

Figure 2. Normalized vertical-component velocity seismograms recorded at MDJ for the seismic event on 9 September 2016, and four confirmed North Korean nuclear tests on 6 January 2016, 12 February 2013, 15 May 2009, and 9 October 2006. The event dates, maximum amplitudes, and epicenter distances are listed on the left. The marks on the waveforms indicate apparent group velocities. These seismograms are characterized by impulsive *P*-wave onsets, relatively weak *Lg* phases, and 3- to 5-s short-period Rayleigh waves.

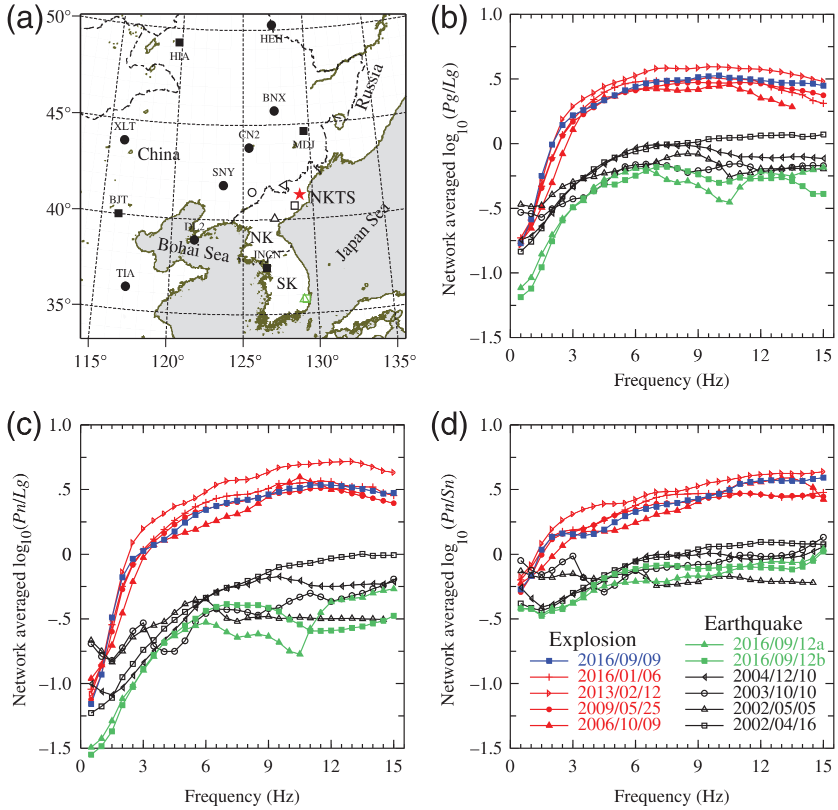

Figure 3. (a) Map showing the location of the NKTS (red star), locations of the stations used for calculating the spectral ratios (solid squares and circles), epicenters of known natural earthquakes (black open symbols), and two unidentified events (green open symbols). (b–d) Network averaged spectral ratios versus frequencies for *Pg*/*Lg*, *Pn*/*Lg*, and *Pn*/*Sn*. The known NKTS explosions are shown in red, the 9 September 2016 event is shown in blue, the known earthquakes are shown in black, and the two events on 12 September 2016 are shown in green.

are spectral ratios calculated for individual stations with network averages and standard deviations indicated by solid lines and shadows. Clearly, the individual station data show large scatters, particularly for smaller or remote events. On the contrast, the network averaged values are far more robust (e.g., Gupta *et al.*, 1992; Kim *et al.*, 1993; Richards and Kim, 2007; Zhao *et al.*, 2008, 2014, 2016). Figure 3b–d shows the network averaged spectral ratios *Pg*/*Lg*, *Pn*/*Lg*, and *Pn*/*Sn* from the four confirmed explosions (NKT1–NKT4, red), four natural earthquakes (black), and three yet-to-be-identified seismic events on 9 (blue) and 12 (green) September 2016. For all three types of spectral ratios, the explosion and earthquake populations can be completely discriminated at frequencies above 2.0 Hz. The 9 September 2016 event at the NKTS falls well within the explosion group and can be confirmed as a new underground nuclear test, whereas the two 12 September 2016 events are unambiguously within the earthquake population.

High-Precision Relative Location

With increasing differential *Pn* travel-time data from the NKTS explosions, the relative location method (Schaff and Richards, 2004; Selby, 2010; Wen and Long, 2010; Murphy *et al.*, 2013; Zhang and Wen, 2013; Zhao *et al.*, 2014, 2016) provides highly accurate event locations relative to a given master event. Following Zhao *et al.* (2014), we use NKT1 as the master event to simultaneously constrain the locations and origin times for NKT2–NKT5. Because the five North Korean nuclear tests were closely detonated, the *Pn* differential travel times at individual stations can be attributed to their origin times, epicentral locations, burial depths, and *Pn* velocity beneath the NKTS. Based on previous investigations, we fix the uppermost-mantle *Pn* velocity to 7.99 km/s (e.g., Zhao *et al.*, 2016). Considering the trade-off between depth and origin time, only the latter is included in the calculation. Finally, we create a relative relocation model with 12 parameters including the longitudes, latitudes, and origin times for NKT2–NKT5 to fit the observed *Pn* differential travel times.

Pn waveforms observed at 197 regional seismic stations (Fig. 1 and Ⓔ Tables S1 and S2) are used for the cross-correlation calculations (Schaff and Richards, 2004; Zhao *et al.*, 2016), which result in 578 differential travel times for relocation modeling (Ⓔ Fig. S3 and Tables S1–S4). The investigated model is parameterized by the longitudes, latitudes, and origin times for NKT2–NKT5 (Table 1). We provide variation ranges of the NKT2–NKT4 parameters based on our previous results (Zhao *et al.*, 2014, 2016). In contrast, a relatively broader range is set for the NKT5 event parameter. Simulated annealing (Kirkpatrick *et al.*, 1983), which is a nonexhaustive global optimization algorithm, is used to estimate the parameters in model space. This method has been widely applied in geophysical modeling (e.g., Kirkpatrick, 1984; Iritani *et al.*, 2014; Zhao *et al.*, 2015). We perform the parameter search by minimizing the L2 norm of the difference between the observed and synthetic *Pn* differential travel times. The best-fit model parameters and their standard deviations are obtained by the bootstrap method (Efron, 1983) and are listed in Table 1. The best-fit epicenter of NKT5 is 41.2976° N, 129.0804° E, which is close to the result provided by Gibbons *et al.* (2017) for the same event. Based on the error ellipses (Allan, 1972), the precision in the relative location is ~32 m (Table 1). In Figure 4, the epicenter of NKT5 is ~1000 m east and 300 m south of NKT4, 200 m east and 300 m north of NKT2, and 2600 and 900 m from NKT1 and NKT3, respectively. NKT5 appeared to occur under the same mountain as NKT2, NKT3, and NKT4, although it is closer to the peak. The best-fit origin time

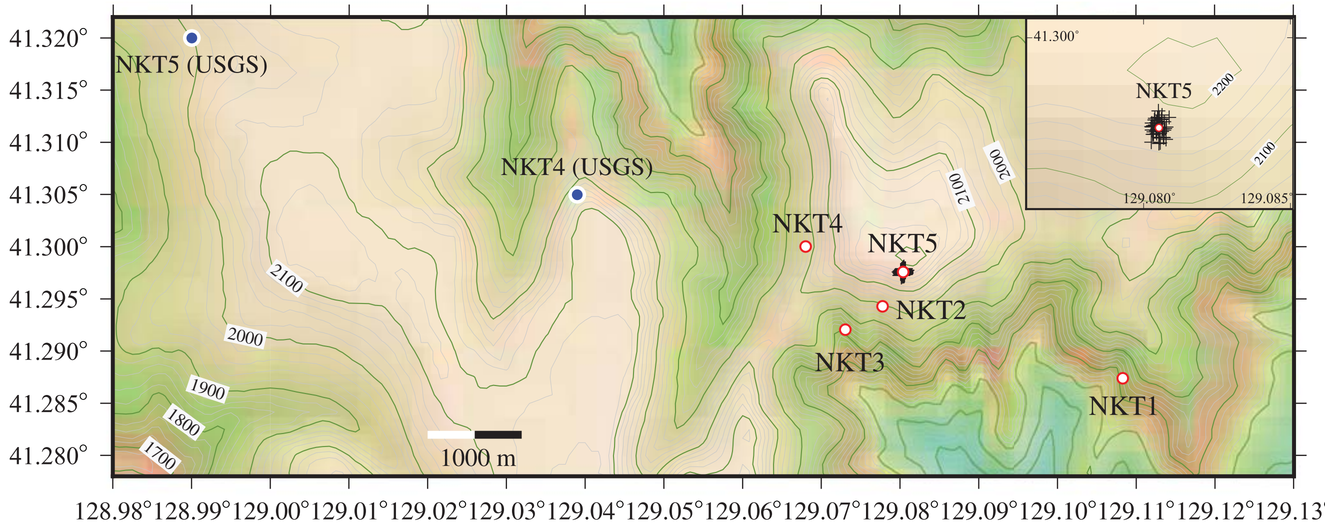

Figure 4. Map showing the topography and relocated epicenters of the NKTS explosions. The white dots are the results from this study, and the blue dots are those given by the U.S. Geological Survey (USGS). The inset map zooms into the source region of the NKT5, where crosses are epicenters obtained using partial information and used to estimate errors based on the bootstrap method (Efron, 1983).

for NKT5 is 00:30:01.3857 ± 0.0014 UTC. The accuracy of the final relocation is strongly dependent on the master event NKT1.

Body- and Surface-Wave Magnitudes

The body- and surface-wave magnitudes are calculated based on an 11-station regional seismic network. The

Table 1
Model Parameters of the *Pn* Differential Travel Times Used in This Study

North Korean Nuclear Test (yyyy/mm/dd)	Model Space and Prior Information					Best-Fit Inverted Model	
	Parameter	Name	Prior Information	Data Range	References	Mean	Standard Deviation
NKT1 (2006/10/09)	x1	Longitude (°E)	129.1083	Fixed as master event	Wen and Long (2010)	129.1083	0
	y1	Latitude (°N)	41.2874		Zhao *et al.* (2014)	41.2874	0
	t01	Origin time (hh:mm:ss.ssss)	01:35:28.0000		USGS	01:35:28.0000	0
	V_{Pn}	*Pn* velocity (m/s)	7.99		Zhao *et al.* (2016)	7.99	0
NKT2 (2009/05/25)	x2	Longitude (°E)	129.0775	x2 ± 0.0030		129.0778	0.0004
	y2	Latitude (°N)	41.2940	y2 ± 0.0030	Zhao *et al.* (2014)	41.2943	0.0005
	t02	Origin time (hh:mm:ss.ssss)	00:54:43.1142	t02 ± 20 (s)	Wen and Long (2010)	00:54:43.1239	0.0027
NKT3 (2013/02/13)	x3	Longitude (°E)	129.0733	x3 ± 0.0030		129.0730	0.0004
	y3	Latitude (°N)	41.2918	y3 ± 0.0030	Zhao *et al.* (2014)	41.2921	0.0005
	t03	Origin time (hh:mm:ss.ssss)	02:57:51.2741	t03 ± 20 (s)	Zhang and Wen (2013)	02:57:51.2725	0.0016
NKT4 (2016/01/06)	x4	Longitude (°E)	129.0678	x4 ± 0.0040		129.0680	0.0005
	y4	Latitude (°N)	41.3003	y4 ± 0.0040	Zhao *et al.* (2016)	41.3001	0.0006
	t04	Origin time (hh:mm:ss.ssss)	01:30:00.9706	t04 ± 20 (s)		01:30:00.9635	0.0014
NKT5 (2016/09/09)	x5	Longitude (°E)	128.9900	x5 ± 0.2000	Gibbons *et al.* (2017)	129.0804	0.0002
	y5	Latitude (°N)	41.3200	y5 ± 0.2000	USGS	41.2976	0.0003
	t05	Origin time (hh:mm:ss.ssss)	00:30:02.0000	t05 ± 20 (s)		00:30:01.3857	0.0014

USGS, U.S. Geological Survey.

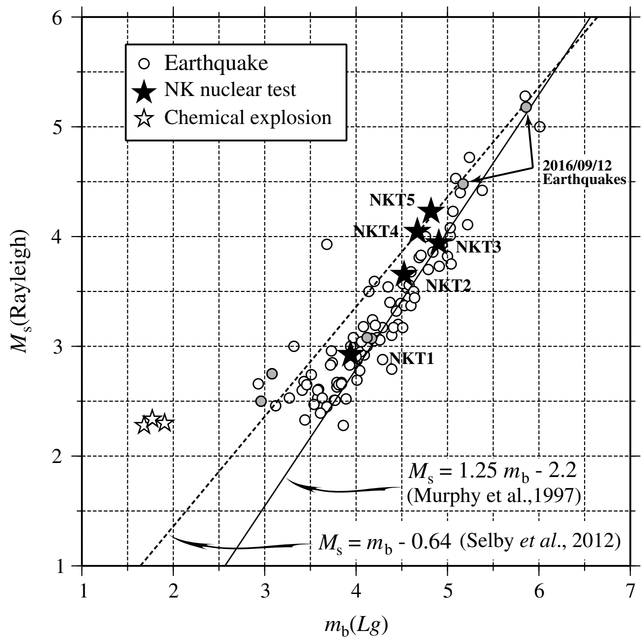

Figure 5. M_s(Rayleigh) versus $m_b(Lg)$ for NKTS explosions (solid stars), natural earthquakes (circles), and chemical explosions (open stars) in northeast China and the Korean Peninsula. The six natural earthquakes used in the identification calculation are filled with light gray color. The solid and dashed lines are the screening criteria provided by Murphy *et al.* (1997) and Selby *et al.* (2012) for separating explosions from earthquakes using the m_b–M_s method.

Lg-wave body-wave magnitudes from the network are precalibrated using a historical dataset composed of 102 regional events with both $m_b(P)$ and $m_b(Lg)$ measurements, and a regional *Lg* attenuation model (Zhao *et al.*, 2008, 2010). Using this network, the body-wave magnitude for NKT5 is $m_b(Lg) = 4.82 \pm 0.18$ (Ⓔ Table S5).

Russell (2006) developed a time-domain surface-wave magnitude measurement method that extends measurements from traditional teleseismic distances to regional distances. Bonner *et al.* (2006) applied this method to multiple datasets to demonstrate its applicability in different regions. For North Korean nuclear tests, several authors used the method and obtained consistent results, either at regional or teleseismic distances (Bonner *et al.*, 2008; Chun *et al.*, 2011; Fan *et al.*, 2013; Murphy *et al.*, 2013). We adopted the method to analyze a group of historical events and calibrate the 11-station regional network for Rayleigh-wave magnitude measurements (Fan *et al.*, 2013). Ⓔ Figure S4 shows an example of surface-wave magnitudes calculated using Rayleigh waves at an individual station. After correcting for the site responses at individual stations and periods, the surface-wave magnitude obtained for NKT5 is $M_s = 4.23 \pm 0.09$ (Table 2 and Ⓔ Table S5). Compared with previous results, the M_s measurements for all NKTS explosions are consistent although different datasets were used (Table 3). Using the 11-station regional network, we obtain the body-wave magnitudes $m_b(Lg)$ and surface-wave magnitudes M_s for all 102 events in northeast China and the Korean Peninsula. The results are illustrated in Figure 5, where the North Korean nuclear tests (solid stars), earthquakes (circles), and three small chemical explosions (open stars) for deep sounding purpose are shown as M_s versus m_b. Two criteria for separating explosions from earthquakes are illustrated (Murphy *et al.*, 1997; Fisk *et al.*, 2002; Selby *et al.*, 2012; Ford and Walter, 2014). The explosion and earthquake populations overlap each other based on the M_s and $m_b(Lg)$ calculated in this study. In particular, the five NKTS explosions and six earthquakes used in the identification calculation (light gray-filled circles) could not be separated properly. At the low magnitude end, the events are further biased from the lines. The results indicate that the *P*/*S* ratio method is a more effective discriminant than the $m_b(Lg)$–M_s difference for explosive source identification on the Korean Peninsula (Bonner *et al.*, 2008; Patton and Taylor, 2008; Selby *et al.*, 2012).

Yield Estimation

The seismic yield of an underground nuclear test can be estimated using a calibrated empirical magnitude–yield

Table 2
Surface-Wave Magnitudes (M_s) of the North Korean Nuclear Tests

	2006/10/09		2009/05/25		2013/02/12		2016/01/06		2016/09/09	
Network. Station	M_s	Period (s)	M_s	Period (s)	M_s	Period (s)	M_s	Period (s)	M_s	Period (s)
HL.BNX	2.54	14	—	—	3.95	14	4.01	14	4.18	9
HL.HEH	—	—	3.56	18	3.80	12	3.96	13	4.13	13
JL.CN2	3.06	18	3.76	8	4.13	8	4.16	8	4.35	8
LN.SNY	3.08	9	3.74	11	4.07	11	4.11	11	4.31	11
LN.DL2	2.87	25	3.67	9	4.05	9	4.14	9	4.36	9
NM.XLT	—	—	—	—	4.02	13	3.98	15	4.18	13
SD.TIA	—	—	—	—	3.59	18	—	—	4.29	18
IC.MDJ	2.78	8	3.60	13	3.83	13	4.00	13	4.19	13
IC.HIA	2.92	19	3.70	11	4.00	10	—	—	4.20	17
IC.BJT	3.01	12	3.59	13	3.98	13	—	—	4.11	14
IC.INCN	3.13	8	3.61	15	—	—	4.02	15	4.20	15
Network average	2.92		3.65		3.94		4.05		4.23	
Standard deviation	0.20		0.07		0.16		0.08		0.09	

Table 3
Comparison of Surface-Wave Magnitudes (M_s) for North Korean Nuclear Tests from Different Authors

2006/10/09	2009/05/25	2013/02/12	2016/01/06	2016/09/09	References
2.94 ± 0.17	—	—	—	—	Bonner *et al.* (2008)
2.8	3.55 ± 0.06	—	—	—	Shin *et al.* (2010)
2.89 ± 0.11	3.52 ± 0.16	—	—	—	Chun *et al.* (2011)
2.93 ± 0.20	3.66 ± 0.10	—	—	—	Murphy *et al.* (2013)
2.92 ± 0.20	3.65 ± 0.07	3.94 ± 0.16	4.05 ± 0.08	4.23 ± 0.09	This study

relation either from body-wave magnitude (Nuttli, 1986; Ringdal *et al.*, 1992; Murphy, 1996; Bowers *et al.*, 2001; Zhao *et al.*, 2008, 2012; Zhang and Wen, 2013) or surface-wave magnitude (e.g., Stevens and McLaughlin, 2001; Stevens and Murphy, 2001; Patton, 2016). Because the nuclear explosion yield of the NKTS is not available, this test site is uncalibrated. To estimate the seismic yield, we borrowed the empirical relation from a calibrated site. The NKTS explosions generated unusually strong Rayleigh waves (Murphy *et al.*, 2013; Zhao *et al.*, 2016), and the resulting surface-wave magnitude may overestimate the yields of NKTS explosions (e.g., Bonner *et al.*, 2008; Stevens and Thompson, 2015; Patton, 2016). Therefore, only the body-wave magnitude from the regional phase *Lg* is used to estimate the seismic yields for the North Korean nuclear tests. Considering that the NKTS is located on a stable platform, we choose empirical magnitude–yield relations for hard-rock regions, that is, those at the test sites Novaya Zemlya (Bowers *et al.*, 2001) and East Kazakhstan (Ringdal *et al.*, 1992; Murphy, 1996). Based on three chemical explosions with known yields (Richards and Kim, 2007; Zhao *et al.*, 2008), we prefer the fully coupled hard-rock site equation by Bowers *et al.* (2001) for the NKTS (Zhao *et al.*, 2008, 2012, 2014, 2016). The estimated yield for NKT5 was 6 kt using this relationship and assuming a normally scaled burial depth. Transferring the ±0.2 magnitude measurement error to the yield introduces uncertainty between 3 and 11 kt. However, this yield could be underestimated if the source is greatly overburied.

Discussion and Conclusions

Based on broadband regional seismic data recorded in northeast China, South Korea, and Japan, we investigated the seismic characteristics of the 9 September 2016 event near the NKTS, and two other seismic events on the Korean Peninsula on 12 September 2016. Based on a regional network analysis, the 9 September 2016 North Korean event was confirmed to be an underground nuclear test, and the two 12 September 2016 events were identified as natural earthquakes. These results indicate that the network-based *P*/*S*-type spectral ratios from regional phases are effective discriminants for separating explosions and earthquakes on the Korean Peninsula. An underground nuclear test detonated in the China–North Korea border area can be unambiguously recognized using a regional seismic network.

The locations and origin times of NKT2–NKT5 were determined based on the relative location method using NKT1 as the master event. The results are consistent with those of previous reports (e.g., Wen and Long, 2010; Zhang and Wen, 2013; Zhao *et al.*, 2014, 2016). However, the current results are calculated based on a local 1D model. There are clues that the regional 3D structure at the source region may affect the relative location result. The error analysis regarding the relocation accuracy does not reflect the errors resulted from the 1D approximation. Recently, Gibbons *et al.* (2017) found that there are discrepancies between the differential travel times measured from the global *P* waves and regional *Pn* waves. They used an optimization method to find compensations to eliminate these discrepancies and improve the accuracy in relative location.

To date, no explosion with known yields has been documented at the NKTS. Therefore, the yield estimation obtained here can be affected by several factors, such as transfer of an empirical magnitude–yield relation from a calibrated test site, replacement of the global $m_b(P)$ with the regional $m_b(Lg)$, unknown burial depths, and local geology, can introduce uncertainties to the yield estimation, and certain factors may cause severe biases. For individual events, specific source mechanisms and near-source environment can cause biases from a general $m_b(P)$–$m_b(Lg)$ relation. For example, NKT4 and NKT5 have 0.1–0.2 magnitude unit differences between $m_b(P)$ and $m_b(Lg)$. To prevent radioactive leakage, the underground nuclear tests used to be overburied. The burial depth may be estimated using the elevation difference between the epicenter and tunnel entrance (e.g., Zhang and Wen, 2013). Based on the relocation results (Fig. 4), the minimum burial depth for NKT5 was ~780 m (Gibbons *et al.*, 2017). If this is the case, a downward extension of 400 m can increase the seismic yield of the NKT5 to between 16 and 22 kt.

Data and Resources

The waveforms recorded at the China National Digital Seismic Network (CNDSN), Global Seismic Network (GSN), and F-NET stations used in this study were collected from the China Earthquake Network Center (CENC), the Data Management Centre of China National Seismic Network at the Institute of Geophysics, the China Earthquake Administration (SEISDMC; Zheng *et al.*, 2010) at http://

www.seisdmc.ac.cn (last accessed September 2016), the Incorporated Research Institutions for Seismology Data Management Center (IRIS-DMC) at www.iris.edu (last accessed September 2016), and the National Research Institute for Earth Science and Disaster Prevention (NIED) at http://www.fnet.bosai.go.jp (last accessed September 2016). The source parameters for the three chemical explosions were provided by X.-K. Zhang at the Geophysical Exploration Center of China Earthquake Administration (GECCEA).

Acknowledgments

The authors thank T. Lay for engaging in discussions on this work. The constructive comments of Associate Editor C. P. Zeiler and three anonymous reviewers greatly improved this article and are appreciated. This research was supported by the National Natural Science Foundation of China (Grants 41674060, 41630210, and 41374065). Certain figures were created using the Generic Mapping Tools (GMT; Wessel and Smith, 1998).

References

Allan, A. L. (1972). The error ellipse: A further note, *Surv. Rev.* **21,** no. 166, 387–390, doi: 10.1179/sre.1972.21.166.387.

Bonner, J., R. B. Herrmann, D. Harkrider, and M. Pasyanos (2008). The surface-wave magnitude for the 9 October 2006 North Korean nuclear explosion, *Bull. Seismol. Soc. Am.* **98,** no. 5, 2498–2506, doi: 10.1785/0120080929.

Bonner, J. L., D. R. Russell, D. G. Harkrider, D. T. Reiter, and R. B. Herrmann (2006). Development of a time-domain, variable-period surface-wave magnitude measurement procedure for application at regional and teleseismic distances, part II: Application and M_s–m_b performance, *Bull. Seismol. Soc. Am.* **96,** no. 2, 678–696, doi: 10.1785/0120050056.

Bonner, J. L., A. Stroujkova, and D. Anderson (2011). Determination of Love- and Rayleigh-wave magnitudes for earthquakes and explosions, *Bull. Seismol. Soc. Am.* **101,** no. 6, 3096–3104, doi: 10.1785/0120110131.

Bowers, D., P. D. Marshall, and A. Douglas (2001). The level of deterrence provided by data from the SPITS seismometer array to possible violations of the Comprehensive Test Ban in the Novaya Zemlya region, *Geophys. J. Int.* **146,** no. 2, 425–438.

Chun, K. Y., Y. Wu, and G. A. Henderson (2011). Magnitude estimation and source discrimination: A close look at the 2006 and 2009 North Korean underground nuclear explosions, *Bull. Seismol. Soc. Am.* **101,** no. 3, 1315–1329, doi: 10.1785/0120100202.

Efron, B. (1983). Estimating the error rate of a prediction rule: Improvement on cross-validation, *J. Am. Stat. Assoc.* **78,** no. 382, 316–331, doi: 10.2307/2288636.

Fan, N., L. F. Zhao, X. B. Xie, and Z. X. Yao (2013). Measurement of Rayleigh-wave magnitudes for North Korean nuclear tests, *Chin. J. Geophys.* **56,** no. 3, 906–915, doi: 10.6038/cjg20130319.

Fisk, M. D. (2006). Source spectral modeling of regional *P*/*S* discriminants at nuclear test sites in China and the former Soviet Union, *Bull. Seismol. Soc. Am.* **96,** no. 6, 2348–2367, doi: 10.1785/0120060023.

Fisk, M. D., D. Jepsen, and J. R. Murphy (2002). Experimental seismic event-screening criteria at the prototype International Data Center, *Pure Appl. Geophys.* **159,** no. 4, 865–888, doi: 10.1007/s00024-002-8662-6.

Ford, S. R., and W. R. Walter (2014). $m_b : M_s$ screening revisited for large events, *Bull. Seismol. Soc. Am.* **104,** no. 3, 1550–1555, doi: 10.1785/0120130182.

Gibbons, S. J., F. Pabian, S. P. Näsholm, T. Kværna, and S. Mykkeltveit (2017). Accurate relative location estimates for the North Korean nuclear tests using empirical slowness corrections, *Geophys. J. Int.* **208,** 101–117, doi: 10.1093/gji/ggw379.

Gupta, I. N., W. W. Chan, and R. A. Wagner (1992). A comparison of regional phases from underground nuclear explosions at East Kazakh and Nevada test sites, *Bull. Seismol. Soc. Am.* **82,** no. 1, 352–382.

Hartse, H. E., S. R. Taylor, W. S. Phillips, and G. E. Randall (1997). A preliminary study of regional seismic discrimination in central Asia with emphasis on western China, *Bull. Seismol. Soc. Am.* **87,** no. 3, 551–568.

Iritani, R., N. Takeuchi, and H. Kawakatsu (2014). Intricate heterogeneous structures of the top 300 km of the Earth's inner core inferred from global array data: II. Frequency dependence of inner core attenuation and its implication, *Earth Planet. Sci. Lett.* **405,** 231–243, doi: 10.1016/j.epsl.2014.08.038.

Kim, W. Y., D. W. Simpson, and P. G. Richards (1993). Discrimination of earthquakes and explosions in the eastern United States using regional high-frequency data, *Geophys. Res. Lett.* **20,** no. 14, 1507–1510, doi: 10.1029/93gl01267.

Kirkpatrick, S. (1984). Optimization by simulated annealing: Quantitative studies, *J. Stat. Phys.* **34,** nos. 5/6, 975–986, doi: 10.1007/Bf01009452.

Kirkpatrick, S., C. D. Gelatt, and M. P. Vecchi (1983). Optimization by simulated annealing, *Science* **220,** no. 4598, 671–680, doi: 10.1126/science.220.4598.671.

Murphy, J. R (1996). Type of seismic events and their source descriptions, in *Monitoring a Comprehensive Test Ban Treaty*, E. S. Husebye and A. M. Dainty (Editors), Kluwer Academic Publishers, Dordrecht, The Netherlands, 225–245.

Murphy, J. R., B. W. Barker, and M. E. Marshall (1997). Event screening at the IDC using the M_s/m_b discriminant, *Maxwell Technologies Final Report*, 23 pp.

Murphy, J. R., J. L. Stevens, B. C. Kohl, and T. J. Bennett (2013). Advanced seismic analyses of the source characteristics of the 2006 and 2009 North Korean nuclear tests, *Bull. Seismol. Soc. Am.* **103,** no. 3, 1640–1661, doi: 10.1785/0120120194.

Nuttli, O. W. (1986). Yield estimates of Nevada test site explosions obtained from seismic *Lg* waves, *J. Geophys. Res.* **91,** no. B2, 2137–2151, doi: 10.1029/Jb091ib02p02137.

Patton, H. J. (2016). A physical basis for M_s-yield scaling in hard rock and implications for late-time damage of the source medium, *Geophys. J. Int.* **206,** no. 1, 191–204, doi: 10.1093/gji/ggw140.

Patton, H. J., and S. R. Taylor (2008). Effects of shock-induced tensile failure on m_b–M_s discrimination: Contrasts between historic nuclear explosions and the North Korean test of 9 October 2006, *Geophys. Res. Lett.* **35,** L14301, doi: 10.1029/2008GL034211.

Richards, P. G., and W. Y. Kim (2007). Seismic signature, *Nature Phys.* **3,** no. 1, 4–6, doi: 10.1038/Nphys495.

Ringdal, F., P. D. Marshall, and R. W. Alewine (1992). Seismic yield determination of Soviet underground nuclear explosions at the Shagan River test site, *Geophys. J. Int.* **109,** no. 1, 65–77, doi: 10.1111/j.1365-246X.1992.tb00079.x.

Russell, D. R. (2006). Development of a time-domain, variable-period surface-wave magnitude measurement procedure for application at regional and teleseismic distances, part I: Theory, *Bull. Seismol. Soc. Am.* **96,** no. 2, 665–677, doi: 10.1785/0120050055.

Schaff, D. P., and P. G. Richards (2004). Repeating seismic events in China, *Science* **303,** no. 5661, 1176–1178, doi: 10.1126/science.1093422.

Schlittenhardt, J., M. Canty, and I. Grunberg (2010). Satellite earth observations support CTBT monitoring: A case study of the nuclear test in North Korea of Oct. 9, 2006 and comparison with seismic results, *Pure Appl. Geophys.* **167,** nos. 4/5, 601–618, doi: 10.1007/s00024-009-0036-x.

Selby, N. D. (2010). Relative locations of the October 2006 and May 2009 DPRK announced nuclear tests using international monitoring system seismometer arrays, *Bull. Seismol. Soc. Am.* **100,** no. 4, 1779–1784, doi: 10.1785/0120100006.

Selby, N. D., P. D. Marshall, and D. Bowers (2012). $m_b : M_s$ event screening revisited, *Bull. Seismol. Soc. Am.* **102,** no. 1, 88–97, doi: 10.1785/0120100349.

Shin, J. S., D. H. Sheen, and G. Kim (2010). Regional observations of the second North Korean nuclear test on 2009 May 25, *Geophys. J. Int.* **180,** no. 1, 243–250, doi: 10.1111/j.1365-246X.2009.04422.x.

Stevens, J. L., and K. L. McLaughlin (2001). Optimization of surface wave identification and measurement, *Pure Appl. Geophys.* **158,** no. 8, 1547–1582, doi: 10.1007/Pl00001234.

Stevens, J. L., and J. R. Murphy (2001). Yield estimation from surface-wave amplitudes, *Pure Appl. Geophys.* **158,** no. 11, 2227–2251, doi: 10.1007/Pl00001147.

Stevens, J. L., and T. W. Thompson (2015). 3D numerical modeling of tectonic strain release from explosions, *Bull. Seismol. Soc. Am.* **105,** no. 2A, 612–621, doi: 10.1785/0120140125.

Taylor, S. R., M. D. Denny, E. S. Vergino, and R. E. Glaser (1989). Regional discrimination between NTS explosions and western United States earthquakes, *Bull. Seismol. Soc. Am.* **79,** no. 4, 1142–1176.

Walter, W. R., E. Matzel, M. E. Pasyanos, D. B. Harris, R. Gok, and S. R. Ford (2007). Empirical observations of earthquake-explosion discrimination using *P*/*S* ratios and implications for the sources of explosion *S*-waves, *29th Monitoring Research Review: Ground-Based Nuclear Explosion Monitoring Technologies*, 684–693.

Walter, W. R., K. M. Mayeda, and H. J. Patton (1995), Phase and spectral ratio discrimination between NTS earthquakes and explosions: 1. Empirical observations, *Bull. Seismol. Soc. Am.* **85,** no. 4, 1050–1067.

Wen, L. X., and H. Long (2010). High-precision location of North Korea's 2009 nuclear test, *Seismol. Res. Lett.* **81,** no. 1, 26–29, doi: 10.1785/gssrl.81.1.26.

Wessel, P., and W. Smith (1998). New, improved version of the generic mapping tools released, *Eos Trans. AGU* **79,** 579.

Xie, J. (2002). Source scaling of *Pn* and *Lg* spectra and their ratios from explosions in central Asia: Implications for the identification of small seismic events at regional distances, *J. Geophys. Res.* **107,** no. B72128, doi: 10.1029/2001JB000509.

Zhang, M., and L. X. Wen (2013). High-precision location and yield of North Korea's 2013 nuclear test, *Geophys. Res. Lett.* **40,** no. 12, 2941–2946, doi: 10.1002/grl.50607.

Zhao, L. F., X. B. Xie, B. F. Tian, Q. F. Chen, T. Y. Hao, and Z. X. Yao (2015). *Pn* wave geometrical spreading and attenuation in Northeast China and the Korean Peninsula constrained by observations from North Korean nuclear explosions, *J. Geophys. Res.* **120,** 7558–7571, doi: 10.1002/2015JB012205.

Zhao, L. F., X. B. Xie, W. M. Wang, J. L. Hao, and Z. X. Yao (2016). Seismological investigation of the 2016 January 6 North Korean underground nuclear test, *Geophys. J. Int.* **206,** 1487–1491, doi: 10.1093/gji/ggw239.

Zhao, L. F., X. B. Xie, W. M. Wang, and Z. X. Yao (2008). Regional seismic characteristics of the 9 October 2006 North Korean nuclear test, *Bull. Seismol. Soc. Am.* **98,** no. 6, 2571–2589, doi: 10.1785/0120080128.

Zhao, L. F., X. B. Xie, W. M. Wang, and Z. X. Yao (2012). Yield estimation of the 25 May 2009 North Korean nuclear explosion, *Bull. Seismol. Soc. Am.* **102,** no. 2, 467–478, doi: 10.1785/0120110163.

Zhao, L. F., X. B. Xie, W. M. Wang, and Z. X. Yao (2014). The 12 February 2013 North Korean underground nuclear test, *Seismol. Res. Lett.* **85,** no. 1, 130–134, doi: 10.1785/0220130103.

Zhao, L. F., X. B. Xie, W. M. Wang, J. H. Zhang, and Z. X. Yao (2010). Seismic *Lg*-wave *Q* tomography in and around Northeast China, *J. Geophys. Res.* **115,** no. B08307, doi: 10.1029/2009JB007157.

Zheng, X. F., Z. X. Yao, J. H. Liang, and J. Zheng (2010). The role played and opportunities provided by IGP DMC of China National Seismic Network in Wenchuan earthquake disaster relief and researches, *Bull. Seismol. Soc. Am.* **100,** no. 5B, 2866–2872, doi: 10.1785/0120090257.

Key Laboratory of Earth and Planetary Physics
Institute of Geology and Geophysics, Chinese Academy of Sciences
19 Beituchengxilu, Chaoyang District
Beijing 100029, China
zhaolf@mail.iggcas.ac.cn
zhaox@mail.iggcas.ac.cn
yaozx@mail.iggcas.ac.cn
(L.-F.Z., X.Z., Z.-X.Y.)

Institute of Geophysics and Planetary Physics
University of California at Santa Cruz
1156 High Street
Santa Cruz, California 95064
xxie@ucsc.edu
(X.-B.X.)

Key Laboratory of Continental Collision and Plateau Uplift
Institute of Tibetan Plateau Research, Chinese Academy of Sciences
16 Lincui Road, Chaoyang District
Beijing 100101, China
Wangwm@itpcas.ac.cn
(W.-M.W.)

Key Laboratory of Exploration Technologies for Oil and Gas Resources
Yangtze University
111 Daxue Road, Caidian District
Wuhan 430100, China
fannachina@hotmail.com
(N.F.)

Manuscript received 16 November 2016;
Published Online 31 October 2017